Journal of Membrane Science 618 (2021) 118727

Contents lists available at ScienceDirect

Journal of Membrane Science

journal homepage: http://www.elsevier.com/locate/memsci

Pressure-modulated synthesis of self-repairing covalent organic frameworks (COFs) for high-flux nanofiltration

Congcong Yin, Siyu Fang, Xiansong Shi, Zhe Zhang, Yong Wang *

State Key Laboratory of Materials-Oriented Chemical Engineering, College of Chemical Engineering, Nanjing Tech University, Nanjing, 211816, PR China

ARTICLE INFO

Keywords:
Covalent organic frameworks (COFs)
Pressure-modulated synthesis
Nanofiltration
Controlled diffusion
Self-repairing

ABSTRACT

Covalent organic frameworks (COFs), with their inherent merits of specific pore size and uniform channels, have been extensively employed to produce nanofiltration (NF) membranes. However, COF-based NF towards precise separations, especially for ion separations, are often unsatisfying due to the intercrystalline defects in selective layers. Herein, a pressure-modulated synthesis method has been explored to prepare crystalline and defect-free COF membranes on seeded substrates for fast NF. Amine and aldehyde solutions are separately placed with a level interval to create vertical hydraulic pressure, which can regulate the mobility of the amine monomers and thus results in the self-repairing of defects in the COF planes and remediation of intercrystalline gaps. The abundant nucleation sites on seeded substrates promote the confined growth of COF crystallites in top layers, leading to an ultrathin selective layer with improved permeance. The resultant COF membrane shows tight methyl orange (~90.4%) and Na_2SO_4 (~63.6%) rejections with a pronounced water permeance of up to ~44.2 L m^{-2} h^{-1} bar^{-1}, which is ~2–10 times higher than other NF membranes with similar rejections. This pressure-modulated synthetic strategy establishes not only the self-repairing synthesis of COFs but also the controllable preparation of defect-free COF-based NF membranes, thus enabling precise and fast separation of molecules and ions.

1. Introduction

Nanofiltration (NF), a burgeoning membrane separation process, has received tremendous attention in wastewater reclamation, desalination, and chemical product purification because of its low energy consumption and high retention of multivalent ions and small molecules (200–1000 Da) [1–6]. In the past decade, researchers have exploited various nanoscale materials to improve the permeance of NF membranes [2,3,7,8]. As an emerging crystalline porous polymer, covalent organic frameworks (COFs) have evolved into promising candidates for the construction of next-generation membranes [8–10]. COFs are featured with a number of distinct superiorities, including well-defined pore apertures down to the sub-nanometer scale, versatile topology architectures, and readily customizable functionalities, making them potent building blocks for NF membranes with superior separation performances [11–14]. Given this, extensive simulation and experimental works on COF-based membranes have been reported, demonstrating their great potential for the separation of pharmaceuticals, dyes, and ions [15–18].

Initially, COFs in the form of particulates were integrated into polymer matrix to produce mixed matrix membranes for gas separation and liquid purification [19,20]. However, the merits of the intrinsic COF pores are hard to take full use because of the discontinuous distribution of COF particles in the polymer matrix [3,6]. Alternatively, researchers attempted to prepare COF membranes by assembling exfoliated COF nanosheets [21,22]. Nevertheless, before membrane preparation, tedious delamination and purification processes are always inevitable to obtain well-dispersed nanosheets [3,6,8]. As a further solution, the bottom-up strategies, such as the solvothermal growth and interfacial reaction, were proposed to prepare COF-based membranes [3,15,18]. For instance, Banerjee and co-workers [23] developed interfacial crystallization to fabricate nanoporous COF films under ambient temperature. Thus-prepared membranes exhibited favorable crystallinity, and showed wide applicability because of their relatively mild synthesis condition. However, despite extensive attempts have been made to prepare COF-based NF membranes, there are only very few reports on COF NF membranes targeting for ion separations. Lai et al. [24] and Mariñas et al. [25] pioneered the preparation of COF membranes for

* Corresponding author.
E-mail address: yongwang@njtech.edu.cn (Y. Wang).

https://doi.org/10.1016/j.memsci.2020.118727
Received 12 July 2020; Received in revised form 15 August 2020; Accepted 6 September 2020
Available online 10 September 2020

desalination by using interfacial polymerization, and they achieved moderate salt rejections. Huang et al. [26] introduced functional groups in COFs to decrease the sieving aperture through post-synthetic modification, thus increasing salt rejection to >80%. Unfortunately, all these membranes exhibited extremely low water permeance, smaller than 1 L m^{-2} h^{-1} bar^{-1}. Very recently, our group employed a COF with a pore size of ~0.9 nm to prepare composite membranes [27]. Thus-prepared membrane showed a Na_2SO_4 rejection of 58.3% and the water permeance was increased to 4.1 L m^{-2} h^{-1} bar^{-1}. The unsatisfactory desalination performances mainly come from the trade-off effect between permeance and selectivity. The difficulties in precisely regulating the synthesis process of COF may lead to the nonselective intercrystalline gaps, i.e., defects, thus weakening selectivity. To reduce defects to the lowest level, thicker selective layers are typically required, in turn leading to greater transport resistance and consequently lower permeance. The COF synthetic strategies discussed above are mainly based on the free reactions between precursors. The restive precursors diffusion leads to the non-ideal growth of COF on the substrates, thus increasing the possibility of defect formation. Therefore, it is highly demanding but remains challenging to precisely control the reaction between precursors to prepare defect-free COF membranes for effective and fast desalination.

Herein, we report a pressure-modulated synthesis strategy to prepare high-quality COF NF membranes with a self-repairing nature to eliminate defects. The external pressure, which comes from the liquid level interval of precursor solutions, provides a dual function for the conformal growth of COF selective layers on porous substrates. First, it suppresses the diffusion of the precursors and promotes the assembly of precursors into distorted frameworks. Second, the nonselective intercrystalline gaps can be effectively eliminated as a result of the well-regulated diffusion rate and the self-repairing process. Meanwhile, abundant nucleation sites on previously seeded substrates promote the confined growth of COF crystals, providing massive transfer paths for water permeation. Therefore, highly crystalline and defect-free selective layers can be prepared, which greatly enhance the molecule and ion rejections while maintain high water permeance.

2. Experimental section

2.1. Materials

1,3,5-Triformylbenzene (TFB) was purchased from Jilin Yanshen Technology Co., Ltd., China. *p*-phenylenediamine (Pa), dioxane and acetic acid were purchased from Aladdin Reagent Co., Ltd. N, N-dimethylformamide (DMF), anhydrous tetrahydrofuran, sodium hydroxide (NaOH), hydrochloric acid, methyl orange (MO), acid fuchsin (AF), Congo red (CR), potassium bromide (KBr) and inorganic salts were obtained from Sinopharm Chemical Reagent Co., Ltd. Polyacrylonitrile (PAN, $M_w = 75$ kDa) was used to prepare the substrates. Deionized (DI) water (conductivity: 2–8 μS cm^{-1}, Wahaha Co.) was used throughout this work. All chemical reagents were commercially available and used without further purification.

2.2. Preparation of hydrolyzed PAN (HPAN) substrates

PAN ultrafiltration membranes were prepared by nonsolvent-induced phase separation. To obtain the casting solution with the concentration of 14 wt%, PAN was dissolved into DMF with the assistance of mechanical stirring at 70 °C for ample time. The homogeneous casting solution was then left in vacuum to degas overnight. Subsequently, the prepared solution was cast on a nonwoven plate with a gap of 200 μm to acquire a casting film, which was then immediately immersed into a coagulation bath of DI water. To obtain the HPAN substrates, the prepared PAN membranes were soaked into 1 M NaOH solution for 20 h at room temperature. Whereafter, the membranes were rinsed with DI water to thoroughly remove the residual NaOH and kept in DI water for 24 h. After that, the membranes were immersed in 1 M hydrochloric acid solution for 2 h at room temperature. All the obtained HPAN substrates were stored in DI water for further use.

2.3. Seeding treatment to HPAN substrates

To prepare precursor solutions for the seeding procedure, 2 mg Pa and 2 mg TFB were separately dissolved in 400 mL dioxane, and 10 μL acetic acid serving as catalyst was then added into the TFB solution. Subsequently, the obtained mixtures were subjected to the ultrasonic treatment to form homogeneous solutions. To prepare the seeding layer, the HPAN substrate was first immersed into the Pa solution for 10 min followed by thoroughly washing with dioxane to remove unreacted Pa. Then, the Pa-grafted HPAN substrate was soaked into the TFB solution for another 10 min to produce the seeded HPAN substrate, which was then rinsed with dioxane. Thus-prepared substrate was stored in DI water before further use. The whole seeding process was carried out at the temperature of 10 °C and humidity of 30%.

2.4. Pressure-modulated synthesis of COFs on seeded HPAN substrates

The pressure-modulated synthesis was developed for the preparation of defect-free COF selective layers on the seeded HPAN substrates to produce separation membranes. Specifically, the seeded substrates were cut into membrane coupons with a diameter of 25 mm and mounted on a home-made cell as shown in Fig. S1. The pipe diameter of the cell is 10 mm and the effective synthesis area is about 3.14 cm^2. In a typical procedure, the seeding layer of the substrates was faced on the TFB solution, and the other side was charged with the Pa solution. Notably, the Pa solution was slowly added into the cell until the liquid level is consistent to the membrane in order to exhaust the air, and then the TFB solution and residual Pa solution were simultaneously poured into the corresponding side of the cell. The pressure-modulated synthesis device was sealed by parafilm and left undisturbed for various durations at room temperature. The obtained COF membrane was gently taken down from the diffusion cell and washed with dioxane for three times to remove unreacted monomers, followed by air drying overnight. To obtain an optimal performance, the Pa/TFB molar ratio was ranged from 8 to 14, and the liquid level interval (Δh) was changed from 0 to 4 cm. For comparison, the COF selective layer was also prepared on the pristine HPAN substrate without a seeding layer following the same synthesizing procedure. As control, free COF particles were also synthesized. A 10 mL glass vial was charged with 0.2 mmol TFB (32 mg) and 2 mL dioxane, followed by sonication for 10 min to obtain a homogeneous precursor solution. Subsequently, 0.3 mmol Pa (32 mg) and 50 μL acetic acid were added, followed by sonication for another 5 min. The vial was then left undisturbed at room temperature for 3 days. The yielded precipitates were collected by vacuum filtration and washed with dioxane and anhydrous tetrahydrofuran for three times. The product was vacuum dried at 120 °C overnight, and then stored in a chamber under constant temperature and humidity (25 °C, 30%) before further characterization.

2.5. Characterizations

The morphology of COF membranes was observed by a field emission scanning electron microscopy (SEM, Hitachi S-4800). Before SEM observations, all samples were sputter-coated with a thin layer of Au/Pd to enhance their conductivity. The X-ray diffraction (XRD) patterns were performed on a Rigaku Smart Lab diffractometer (Cu Kα radiation, λ = 0.15418 nm) at room temperature with the scanning range of 2–40° and scanning rate of $0.01^\circ \cdot s^{-1}$ (voltage = 40 kV, current = 40 mA). Fourier transform infrared (FTIR) spectra were collected on a Nicolet 8700 spectrometer with the wavenumber in the range of 400–4000 cm^{-1}. KBr pressed dish was used for pulverous tests and attenuated total reflection (ATR) mode was used for membrane tests. To avoid the water vapor

during FTIR measurement, the samples were prepared under the exposure of infrared lamp and then tested immediately. The surface roughness of the COF membranes was acquired by an atomic force microscope (AFM, XE-100, Park systems) at non-contact mode.

2.6. Evaluation of NF performances

The water permeance and rejection performance of different membranes were measured by a stirred dead-end filtration cell (Amicon 8003, Millipore) under the operating pressure of 2 bar. A salt aqueous solution (1000 mg L^{-1}) or a dye aqueous solution (50 mg L^{-1}) was used as the feed solution to test the NF performance. Before permeance test, the membranes were pressurized for at least 10 min until reaching a steady state. The water permeance (L m^{-2} h^{-1} bar^{-1}) was defined by normalizing the volume (L) of the permeation through the effective area of A (m^2) during the time t (h) under the trans-membrane pressure P (bar). The concentrations of dye molecules and salts in the feed and filtrate were determined by a UV–Vis spectrophotometer (Nanodrop 2000c, Thermo Fisher Scientific) and a conductivity meter (S230–K, Mettler-Toledo), respectively.

3. Results and discussion

3.1. Pressure-modulated synthesis of COF-LZU1 membranes

The imine-linked COFs are normally synthesized by Schiff base condensation between amine and aldehyde groups [3,9]. Strong covalent bonds and van der Waals forces in intra- and interlayers endow the framework with outstanding stability, which enables the stability of imine bonds in COF-LZU1 membranes [3,18,26]. Here, the introduction of aldehyde-rich seeds can promote the heterogeneous nucleation and growth of the COFs on porous substrates [28]. The seeds were first prepared on HPAN substrates by alternatively immersing the substrate into precursor solutions (Fig. S2). The seeding layer can serve as a barrier to prevent uncontrollable diffusion of precursor pairs. Moreover, it contributes to the formation of nucleation sites for the conformal growth of COF crystals in the HPAN skin layer [29]. After the preparation of seeding layers, COF membranes were fabricated through the pressure-modulated synthesis as shown in Figs. 1a and S1. In this procedure, the precursor solutions containing TFB and Pa are separated on each side of the seeded substrate, and the liquid level of Pa is designed to be higher than that of TFB to form a liquid level interval, which is the definition of Δh. Thus, Pa molecules will be the first to diffuse into the HPAN substrate under the drive of vertical pressure. Subsequently, the Pa molecules are immobilized in the channels due to the interaction between amine groups in Pa and aldehyde groups in pre-synthesized seeds. Upon the permeation of TFB molecules into the skin layer, the condensation occurs with the growth of COF crystals in this nano-confined space (Fig. 1b). Notably, regardless of the position of the Pa solution, the COF particulates produced with the growth of separation layers always generate on the lower liquid level, revealing the regulation of vertical pressure during synthesis. Under the strong actuation of pressure, Pa molecules prefer to permeate into the HPAN skin layer through relatively big channels, which will offer a lower mass transfer resistance. That is, areas with observable cracks and intercrystalline defects can be remediated during the pressure-modulated diffusion process (Fig. 1c), thus providing the formed COF layers with high crystallinity. As a result, the introduction of additional pressure enables the generation of an integrated COF selective layers.

The chemical composition of various samples, including the monomers, seeded substrate, COF-grown membrane and powders, was confirmed by FTIR spectra. As shown in Figs. 2a and S2, the seeded substrate and COF membrane have characteristic peaks at 2247 cm^{-1} and 1734 cm^{-1}, which can be ascribed to the stretching vibrations of cyano and carboxyl groups, respectively. The FTIR spectrum of COF powders exhibits an intense –C═N stretching band at 1620 cm^{-1}, indicating the formation of imine bonds [29]. Additionally, a characteristic absorption peak at the same position can be observed in the spectrum of the seeded substrate and resulting membrane (Fig. 2a, Fig. S3), which demonstrates the formation of COF seeding layers and selective layers. It was also noted that the disappearance of –N-H stretching band (3209-3381 cm^{-1}) of Pa and –C═O stretching (1692 cm^{-1}) of TFB confirms the complete consumption of precursors. Though the membranes and powders were synthesized at room temperature for a relatively short duration, the intense peaks in XRD patterns reveal the high crystallinity of formed COFs (Fig. 2b). The diffraction peak at ~4.7° corresponds to the intrinsic (100) crystallographic plane of COFs [30]. Here, the attenuation in the peak intensity of COF membrane can be easily understood as very few crystals are generated in the substrate channels. The large thickness (>50 μm) of HPAN substrates may also weaken the intensity of peaks during the XRD measurement. Compared with other COF-based separation membranes synthesized at room temperature [31–34], the COF membrane produced by our strategy still presents a higher crystallinity, revealing its highly ordered structure. Evidently, this advantage is originated from the self-repairing process under the regulation of pressure, and could promise a precise molecular sieving performance during membrane separations.

3.2. Microstructures of COF membranes

The morphologies of pressure-modulated synthesized COF membranes were studied by SEM and AFM. As discussed above, the presence

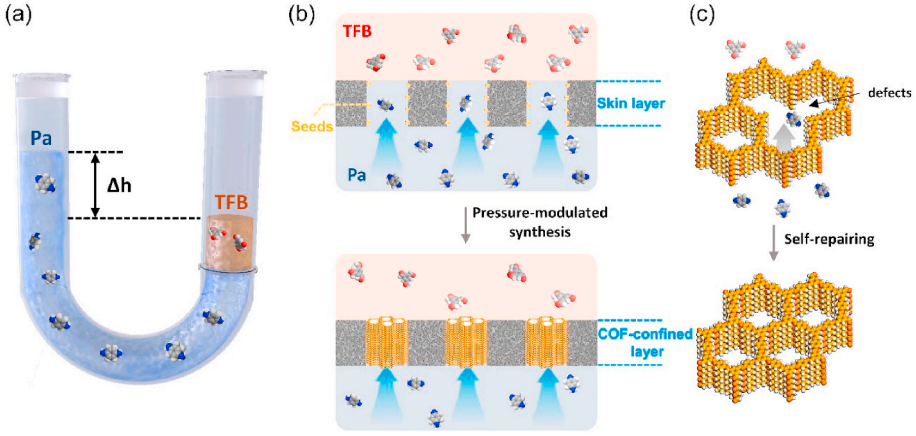

Fig. 1. Scheme of the pressure-modulated synthesis of COF membranes. (a) The vertical diffusion device for membrane growth; (b) schematic diagram of the pressure-modulated synthesis process; (c) the self-repairing process during selective layer formation.

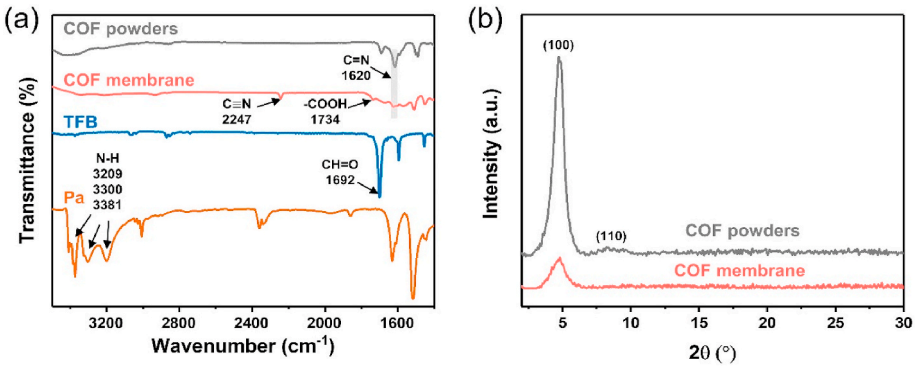

Fig. 2. Structural characterizations. (a) FTIR spectra of the TFB, Pa, COF powders and as-synthesized membrane; (b) XRD patterns of COF powders, and the membrane synthesized for 24h.

of seeding layers can prevent a rapid permeation of Pa into the TFB solution on the opposite side and promote the conformal growth of crystals in the substrate channels. As shown in Figs. 3a and S4, the nano-sized pores can be clearly observed on the COF membrane after synthesizing for a long duration of 72 h on the seeding-free substrate, while the surface nanopores of seeded substrate are completely filled with COF crystals after only 12 h (Fig. S5c). The color of the substrate turns brown after the growth of COFs (Fig. 3b), indicating that crystals are uniformly grown onto the substrate. The surface SEM images show that defect-free COF layers with well-intergrown grains are formed without cracks, pinholes, or other defects (Fig. 3c, Fig. S5). Interestingly, we do not observe a composite structure containing a continuous COF layer from the cross-sectional morphologies (Fig. 3d and e). This result implies that the COF crystals are conformally implanted in the nanoporous skin layer of the HPAN substrate, which leads to the generation of COF-nanoconfined composite membranes [29]. In this case, the COF crystals are discontinuously distributed in the top layer to block the initial nanopores of HPAN substrates. Given the high porosity of skin layers, massive microporous-enriched COF crystals could be embedded, offering plenty of mass transfer paths for water permeation while repelling larger molecules during separations. Without the driving force of pressure ($\Delta h = 0$), observable nanopores appeared on the membrane surface after synthesizing for 24 h, which would greatly reduce the selectivity of membranes (Fig. S6). This is due to the absence of self-repairing process under this pressure-free condition, in which the free diffusion of precursors occurs without a directional growth of crystals to fill these nanopores. With the increase of vertical pressure, the nanopores of seeded substrates are covered with COF crystals, reflecting the significance of external driving force in the preparation of high-quality COF membranes (Fig. S7). Meanwhile, the variation of Pa/TFB molar ratio shows a slight effect on the morphology of COF membranes (Fig. S8). Moreover, the extension of synthesis durations leads to a gradual increase in the surface roughness, as given in Fig. 3f, Fig. S9 and Fig.S10. With the synthesis process proceeding, COFs will grow out from the interior of nanopores to generate crystals on the surface, and these crystals are subsequently combined with their neighbors to form bigger crystals, thus increasing the surface roughness.

3.3. *Influence of synthesis parameters on membrane performances*

Separation performance of the COF membranes was measured by using MO ($M_w = 327$ Da, size $= 1.13 \times 0.42 \times 0.61$ nm^3) dyed water as the feed in a dead-end filtration cell. In the pressure-modulated synthesis of membranes, the control over Δh is critical as the vertical

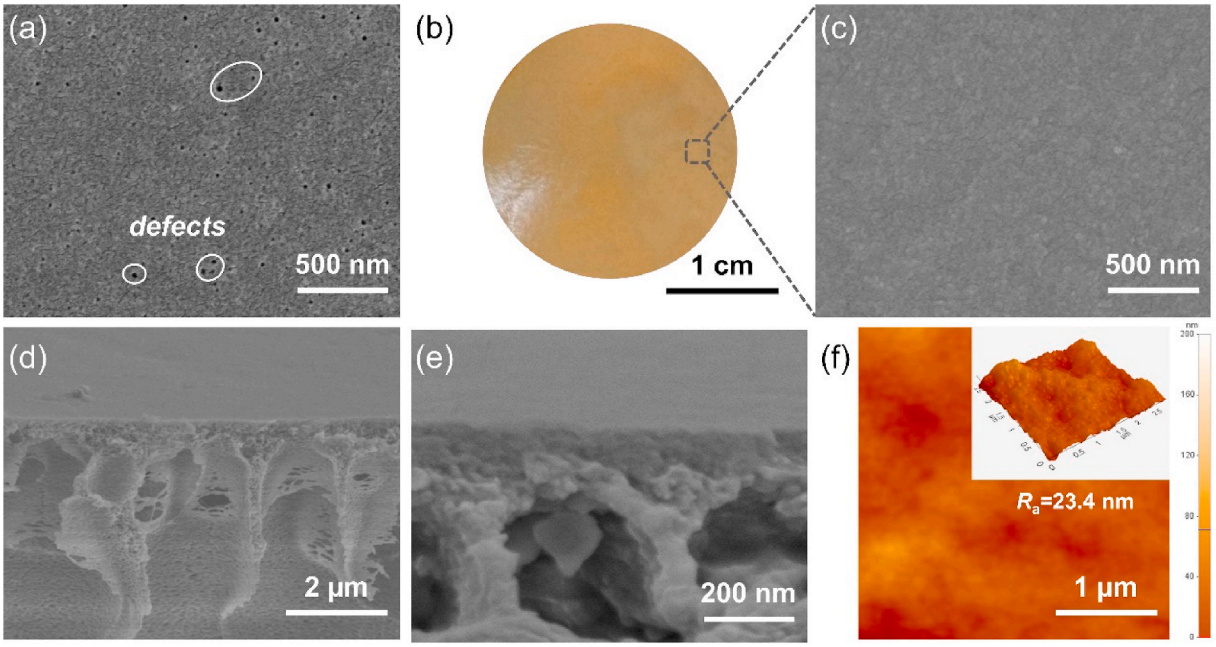

Fig. 3. Morphologies of the COF membranes. (a) Surface SEM image of the membrane synthesized for 72 h without seeds; optical image (b), surface (c), cross-sectional morphologies (d, e), and AFM topography image (f) of the COF membrane synthesized for 24 h.

pressure provides the driving force for the governable diffusion of Pa molecules, triggering the defect self-repairing process and effective elimination of intercrystalline gaps. Here, the regulation on Δh was first studied by varying the liquid level of the Pa solution with a constant concentration and duration (24h), and the corresponding variation of separation performance is given in Fig. 4a. With the absence of vertical pressure (Δh = 0), the synthesized COF membrane shows a relatively high water permeance of 192.4 L m^{-2} h^{-1} bar^{-1}, but the rejection of MO remains a low level of ~31.2%. This inferior performance is corresponding to the observation of the defective structure (Fig. S6), as the nanopores on the surface allow the unobstructed permeation of both water and MO. With the introduction of a low Δh (1 cm), the rejection is greatly increased to ~71.2%, accompanied by a reduced water permeance of ~69.7 L m^{-2} h^{-1} bar^{-1}. Rising the Δh from 1 to 3 cm results in a gradual increase in the rejection. Specifically, the rejections of MO are significantly improved to ~79.3% and ~90.4% when the Δh comes to 2 cm and 3 cm, respectively. The water permeance is slightly decreased from ~51.4 L m^{-2} h^{-1} bar^{-1} to ~44.2 L m^{-2} h^{-1} bar^{-1}. However, a slight decline in the rejection is observed when the Δh keeps rising to 4 cm. Here, we speculate that under this Δh, the Pa molecules may permeate through the substrate into the TFB solution too fast, and there is no sufficient time for the complete elimination of intercrystalline defects. A slight increase in water permeance to ~50.2 L m^{-2} h^{-1} bar^{-1} also evidences the proposed speculation. It is worth noting that the membrane synthesized with the assistance of pressure at room temperature delivers a much higher rejection and comparable permeance than the membrane constructed by the same COF (COF-LZU1, rejection to MO<30%) through the aggressive solvothermal synthesis under a high temperature (120 °C) [35], indicating the advantage of pressure-modulated synthesis in engineering COF-based membranes with enhanced selectivities. Considering the balance between water permeance and rejection, the optimal Δh is believed to be 3 cm, which endows the resultant COF membrane with a pronounced separation performance.

In addition to the determining factor of Δh, the concentration gradient also has an important effect on the property of the COF membranes. In this work, the permeation and selectivity were also investigated by regulating the molar ratio of Pa/TFB in the range of 8–14. When the molar ratio is varied from 8 to 14, the water permeance of COF membranes gradually decreases from ~57.6 L m^{-2} h^{-1} bar^{-1} to 37.2 L m^{-2} h^{-1} bar^{-1}, as shown in Fig. 4b. In addition, the MO rejection rises from ~65.7% to ~90.4% and then decreases to ~82.2%. Here, the variation of MO rejection can be explained by the nucleation-elongation mechanism [36], which mainly relies on the concentration difference of precursor pairs. When applying an appropriate concentration gradient between Pa and TFB, the nanopores of HPAN skin layer will be gently charged with COF crystals to form a nanoconfined composite selective layer for separations. On the contrary, abundant of metastable oligomers would be generated as the nucleation dominating over the crystal growth under an extremely high molar ratio. Besides, the excessive addition of Pa may cause a precursor residual in the skin layer. The space initially occupied by these soluble oligomers and precursors will turn into nonselective defects after washing, giving a slight decline in the rejection. Therefore, the molar ratio of 12 is considered as the optimum condition, and will be utilized as the synthesis parameter for the following investigation.

The synthesis duration is also critical for the preparation of COF membranes as the synthesis duration determines the amount of COF crystallites. As can be seen from Fig. 4c, the COF membrane synthesized for 6 h shows a water permeance of ~96.3 L m^{-2} h^{-1} bar^{-1} with a MO rejection rate of ~78.3%. This moderate separation performance is ascribed to the incomplete padding of nanopores on the surface (Fig. S5b). As the synthesis duration extended, more pronounced molecular sieving behavior can be observed. For instance, with a synthesis duration of 24 h, the membrane exhibits a permeance of ~44.2 L m^{-2} h^{-1} bar^{-1} with a ~90.4% rejection to MO. Further increasing the synthesis duration to 48 and 72 h, the water permeance is remarkably reduced to ~31.4 L m^{-2} h^{-1} bar^{-1} and ~25.4 L m^{-2} h^{-1} bar^{-1}, while the rejection maintains basically unchanged. Obviously, the permeance of membranes continuously decreases with the extension of preparation durations, and a visible change in the separation performance happens during the first 24 h of synthesis. This phenomenon suggests that the primary generated COFs could be nano-sized crystals, which only locate in the nanoporous skin layer of HPAN substrate. The extension on the synthesis duration facilitates the growth of COF crystals on the membrane surface to make COF layer thicker, which is also demonstrated by the increase of surface roughness after prolonging synthesis duration (Fig. S10). As a consequence, the mass transfer resistance is increased

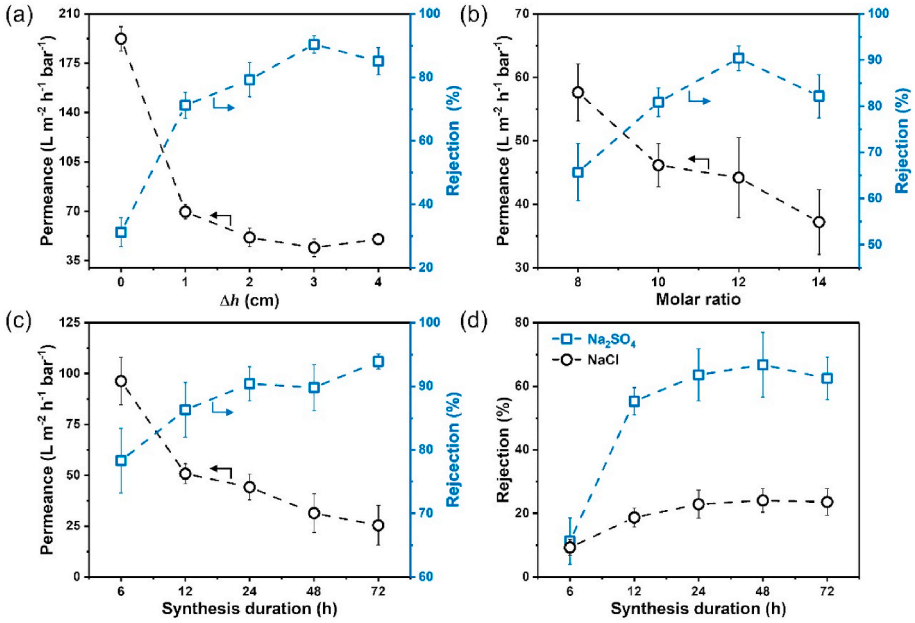

Fig. 4. Membrane performance optimization. Synthesis parameters of Δh (a), Pa/TFB molar ratio (b), and synthesis duration (c) on the COF membrane performance; (d) influence of synthesis duration on ionic sieving.

with the formation of a thicker COF layer, causing a continuous decrease in water permeance. Thus, the optimal synthesis parameter is realized and given as follows: Δh = 3 cm; Pa/TFB molar ratio = 12; synthesis duration = 24 h.

With an offset eclipsed structure, COF-LZU1 possesses inherent pores with a size of ~1.2 nm[30], and the long axial dimension of MO molecule is about 1.13 nm37 (Table S1). The similar size indicates that size-based sieving plays a pivotal character in the precise molecular separations. Given this relatively small pore size and structural integrity, we thought to apply the optimized COF membrane to separate ions from water. As shown in Fig. 4d, the rejection of Na_2SO_4 increases from ~11.3% to ~63.6% with the synthesis duration prolonged from 6 h to 24 h. The rejection rate remains basically unvaried when further extending the synthesis duration. The rejection mechanism can be explained by a synergistic effect of steric hindrance and Donnan exclusion [31–33]. Due to the different valence and hydrated diameter of Cl^- and SO_4^{2-} (Table S2), a high rejection rate to Na_2SO_4 while a relatively low rejection to NaCl are achieved. The noticeable difference between Na_2SO_4 and NaCl rejections also can be frequently observed in the traditional polyamide (PA) NF membranes prepared by interfacial polymerization [38,39]. Owing to their highly ordered pores and desired stability, COFs are receiving great attention in engineering advanced NF membranes for ion separations. A few efforts have been devoted to fabricate COF-based NF membranes to separate ions from water [26,27]. Unfortunately, most of them show relatively low water permeances though they hold comparable ion rejections. Compared to PA-based membranes, the structural benefits of COFs presented in these works are not fully extracted. Our membranes prepared by pressure-modulated synthesis show high performance than that of other COF-based membranes for desalination. This is mainly because of the suppressed precursors mobility and self-repairing process, which leads to a highly crystalline selective layer without defects, enabling tight and fast ion separations.

3.4. Separation performance of optimized COF membranes

To determine the effective pore size of optimized COF membrane by evaluating its molecular weight cut off [35,40], another two dyes, AF (M_w = 586 Da, size = 1.17 × 1.13 × 1.13 nm^3) and CR (M_w = 697 Da, size = 2.56 × 0.73 × 1.13 nm^3), were also applied as detection molecules. By combining separation performances discussed above, the sieving result obtained from various dyes and ions is summarized in Fig. 5. We should note that the effective sizes of these objects are given with their long axial dimensions or hydrated diameters in water (Tables S1 and S2). Clearly, the rejection to dye molecules with sizes ranging from ~1.1 to 2.56 nm is considerably high (>90%), giving an exponentially sharp cutoff at about 1.1 nm. Moreover, species with a size above ~1.17 nm can be effectively removed with a rejection >99%. The stability test was also conducted in a 6 h filtration duration and our membrane showed a very stable MO rejection rate, which is attributed to the structural stability of COF-LZU1 (Fig. S11). Meanwhile, the water permeance is linearly correlated with the operating pressure ranging from 1 to 4 bar, indicating the great pressure resistance of the COF membrane (Fig. S12). The static adsorption result exhibits that the concentration of MO is nearly unchanged after the adsorption measurement, reflecting the great antifouling property of the COF membrane (Fig. S13). This excellent selectivity definitely originates from the well-ordered and defect-free COF transporting channels enabled by pressure-modulated synthesis. Meanwhile, the offset eclipsed structure, which reduces the membrane sieving size to some degree, may also contributes to this pronounced separation performance [30].

In order to highlight the remarkable performance, we then compared the sieving performance of our synthesized COF membranes with other previously reported membranes fabricated by various precursor materials, including COFs, MOFs, nanosheets, and polymers (Table S3). As shown in Fig. 6, although satisfactory permeance or MO rejection of some membranes report in literature, our membrane shows simultaneously high permeance and high MO rejection, with the best comprehensive performance. Importantly, among these NF membranes the COF membrane synthesized in this work also exhibits appreciable rejection performance to Na_2SO_4, and the permeance is ~2–10 times higher than most of other membranes, demonstrating the capability of COF membranes prepared by pressure-modulated synthesis for desalination.

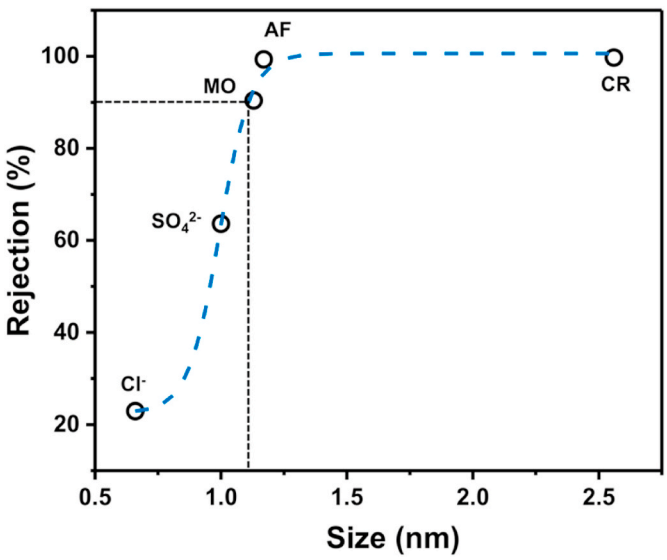

Fig. 5. Rejection of COF membrane to various molecules and ions.

4. Conclusions

In summary, we establish a pressure-modulated strategy to fabricate defect-free COF membranes with high crystallinity. The vertical pressure introduced in the synthesis enables the self-pairing process of intercrystalline defects, endowing the resultant COF membranes with significantly enhanced molecular and ionic sieving capability. Besides, the seeding layer promotes the heterogeneous nucleation and conformal growth of COF crystals, creating an ultrathin selective layer. The synthesis parameters, including liquid level interval (Δh), concentration gradient, and synthesis duration, exhibit a great effect on the membrane performance and are optimized. Thus-obtained COF membrane achieves an excellent molecular sieving performance with water permeance of up to ~44.2 L m^{-2} h^{-1} bar^{-1} as well as outstanding rejections (>90%) to objects with a size above 1.1 nm. Moreover, with such a high water permeance the COF membrane also realizes a satisfactory desalination performance. Considering the facile synthesis of imine-based COFs, this work therefore opens a new avenue for producing tight COF membranes with sharp selectivities, especially for the COFs with sub-nanometer pore sizes towards high-efficiency desalination.

CRediT authorship contribution statement

Congcong Yin: Methodology, Investigation, Writing - original draft, Data curation. **Siyu Fang:** Investigation, Methodology. **Xiansong Shi:** Writing - review & editing, Validation. **Zhe Zhang:** Writing - review & editing. **Yong Wang:** Conceptualization, Supervision.

Declaration of competing interest

The authors declare that they have no known competing financial interests or personal relationships that could have appeared to influence the work reported in this paper.

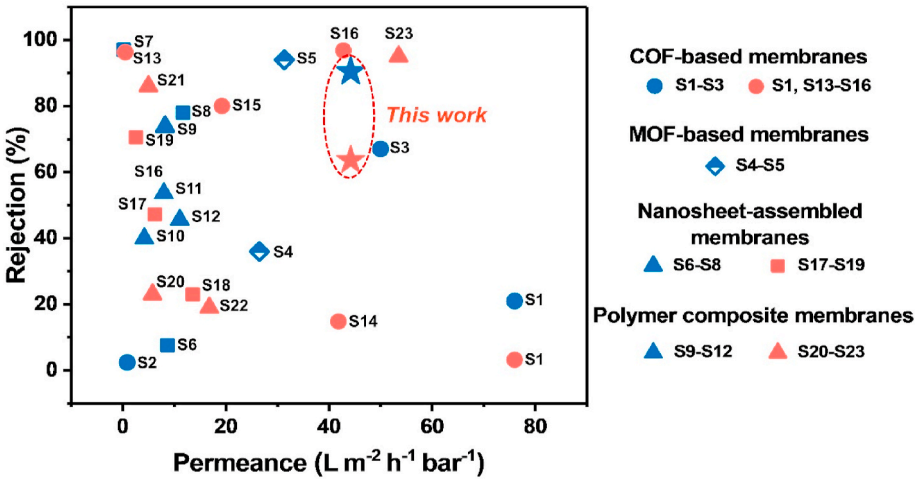

Fig. 6. Comparison of separation performances between our membranes and various reported membranes (blue codes: MO, red codes: Na_2SO_4). (For interpretation of the references to color in this figure legend, the reader is referred to the Web version of this article.)

Acknowledgements

Financial supports from the National Science Foundation of China (21825803, 21921006) are acknowledged. We thank the Program of Excellent Innovation Teams of Jiangsu Higher Education Institutions and the Project of Priority Academic Program Development of Jiangsu Higher Education Institutions (PAPD) for support. We are also grateful to Postgraduate Research & Practice Innovation Program of Jiangsu Province (KYCX20_1097)

Appendix A. Supplementary data

Supplementary data to this article can be found online at https://doi.org/10.1016/j.memsci.2020.118727.

References

[1] V. Pieter, E.M. Lieven, F.J. Ivo, Solvent resistant nanofiltration: separating on a molecular level, Chem. Soc. Rev. 37 (2008) 365–405.

[2] B. Liang, X. He, J.J. Hou, L.S. Li, Z.Y. Tang, Membrane separation in organic liquid: technologies, achievements, and opportunities, Adv. Mater. 31 (2018), 1806090.

[3] S.S. Yuan, X. Li, J.Y. Zhu, G. Zhang, P.V. Puyvelde, B.V.D. Bruggen, Covalent organic frameworks for membrane separation, Chem. Soc. Rev. 48 (2019) 2665–2681.

[4] Y. Han, Z. Xu, C. Gao, Ultrathin graphene nanofiltration membrane for water purification, Adv. Funct. Mater. 23 (2013) 3693–3700.

[5] C.C. Yin, L.L. Dong, Z.G. Wang, M.Q. Chen, Y. Wang, Y. Zhao, CO_2-responsive graphene oxide nanofiltration membranes for switchable rejection to cations and anions, J. Membr. Sci. 592 (2019), 117374.

[6] C. Zhang, B.H. Wu, M.Q. Ma, Z.K. Wang, Z.K. Xu, Ultrathin metal/covalent-organic framework membranes towards ultimate separation, Chem. Soc. Rev. 48 (2019) 3811–3841.

[7] N.B. Mckeown, P.M. Budd, Polymers of intrinsic microporosity (PIMs): organic materials for membrane separations, heterogeneous catalysis and hydrogen storage, Chem. Soc. Rev. 35 (2006) 675–683.

[8] S. Kandambeth, K. Dey, R. Banerjee, Covalent organic frameworks: chemistry beyond the structure, J. Am. Chem. Soc. 141 (2019) 1807–1822.

[9] K. Geng, T. He, R.Y. Liu, K.T. Tan, Z.P. Li, S.S. Tao, Y.F. Gong, Q.H. Jiang, D. L. Jiang, Covalent organic frameworks: design, synthesis, and functions, Chem. Rev. (2020), https://doi.org/10.1021/acs.chemrev.9b00550.

[10] P. Wang, X.Y. Chen, Q.H. Jiang, M. Addicoat, N. Huang, S. Dalapati, T. Heine, F. W. Huo, D.L. Jiang, High-precision size recognition and separation in synthetic 1D nanochannels, Angew. Chem. Int. Ed. 58 (2019) 15922–15927.

[11] S.Y. Ding, W. Wang, Covalent organic frameworks (COFs): from design to applications, Chem. Soc. Rev. 42 (2013) 548–568.

[12] A.P. Cote, A.I. Benin, N.W. Ockwig, M. O'Keeffe, A.J. Matzge, O.M. Yaghi, Porous, crystalline, covalent organic frameworks, Science 310 (2005) 1166–1170.

[13] P.J. Waller, F. Gandara, O.M. Yaghi, Chemistry of covalent organic frameworks, Acc. Chem. Res. 48 (2015) 3053–3063.

[14] V.A. Kuehl, J. Yin, P.H.H. Duong, B. Mastorovich, B. Newell, K.D. Li-Oakey, B. A. Parkinson, J.O. Hoberg, A highly ordered nanoporous, two-dimensional covalent organic framework with modifiable pores, and its application in water purification and ion sieving, J. Am. Chem. Soc. 140 (2018) 18200–18207.

[15] Y. Li, Q.X. Wu, X.H. Guo, M.C. Zhang, B. Chen, G.Y. Wei, X. Li, X.F. Li, S.J. Li, L. J. Ma, Laminated self-standing covalent organic framework membrane with uniformly distributed subnanopores for ionic and molecular sieving, Nat. Commun. 11 (2020) 599.

[16] W. Zhou, M.J. Wei, X. Zhang, F. Xu, Y. Wang, Fast desalination by multilayered covalent organic framework (COF) nanosheets, ACS Appl. Mater. Interfaces 11 (2019) 16847–16854.

[17] C. Yuan, X.W. Wu, R. Gao, X. Han, Y. Liu, Y.T. Long, Y. Cui, Nanochannels of covalent organic frameworks for chiral selective transmembrane transport of amino acids, J. Am. Chem. Soc. 141 (2019) 20187–20197.

[18] Y.P. Ying, M.M. Tong, S.C. Ning, S.K. Ravi, S.B. Peh, S.C. Tan, S.J. Pennycook, D. Zhao, Ultrathin two-dimensional membranes assembled by ionic covalent organic nanosheets with reduced apertures for gas separation, J. Am. Chem. Soc. 142 (2020) 4472–4480.

[19] Z.X. Kang, Y.W. Peng, Y.H. Qian, D.Q. Yuan, M.A. Addicoat, T. Heine, Z.G. Hu, L. Tee, Z.G. Guo, D. Zhao, Mixed matrix membranes (MMMs) comprising exfoliated 2D covalent organic frameworks (COFs) for efficient CO_2 separation, Chem. Mater. 28 (2016) 1277–1285.

[20] C.B. Wang, Z.Y. Li, J.X. Chen, Z. Li, Y.H. Yin, L. Cao, Y.L. Zhong, H. Wu, Covalent organic framework modified polyamide nanofiltration membrane with enhanced performance for desalination, J. Membr. Sci. 523 (2017) 273–281.

[21] G. Li, K. Zhang, T. Tsuru, Two-dimensional covalent organic framework (COF) membranes fabricated via the assembly of exfoliated COF nanosheets, ACS Appl. Mater. Interfaces 9 (2017) 8433–8436.

[22] H. Yang, L.X. Yang, H.J. Wang, Z. Xu, Y.M. Zhao, Y. Luo, N. Nasir, Y.M. Song, H. Wu, F.S. Pan, Z.Y. Jiang, Covalent organic framework membranes through a mixed-dimensional assembly for molecular separations, Nat. Commun. 10 (2019) 2101.

[23] K. Dey, M. Pal, K.C. Rout, H.S. Kunjattu, A. Das, R. Mukherjee, U.K. Kharul, R. Banerjee, Selective molecular separation by interfacially crystallized covalent organic framework thin films, J. Am. Chem. Soc. 139 (2017) 13083–13091.

[24] I. Gadwal, G. Sheng, R.L. Thankamony, Y. Liu, H.F. Li, Z.P. Lai, Synthesis of sub-10 nm two-dimensional covalent organic thin film with sharp molecular sieving nanofiltration, ACS Appl. Mater. Interfaces 10 (2018) 12295–12299.

[25] L. Valentino, M. Matsumoto, W.R. Dichtel, B.J. Marinas, Development and performance characterization of a polyimine covalent organic framework thin-film composite nanofiltration membrane, Environ. Sci. Technol. 51 (2017) 14352–14359.

[26] C. Liu, Y.Z. Jiang, A. Nalaparaju, J.W. Jiang, A.S. Huang, Post-synthesis of a covalent organic framework nanofiltration membrane for highly efficient water treatment, J. Mater. Chem. 7 (2019) 24205–24210.

[27] R. Wang, M.J. Wei, Y. Wang, Secondary growth of covalent organic frameworks (COFs) on porous substrates for fast desalination, J. Membr. Sci. 604 (2020), 118090.

[28] Y.X. Hu, J. Wei, Y. Liang, H.C. Zhang, X.W. Zhang, W. Shen, H.T. Wang, Zeolitic imidazolate framework/graphene oxide hybrid nanosheets as seeds for the growth of ultrathin molecular sieving membranes, Angew. Chem. Int. Ed. 55 (2016) 2048–2052.

[29] N.X. Wang, X.T. Li, L. Wang, L.L. Zhang, G.J. Zhang, S.L. Ji, Nanoconfined zeolitic imidazolate framework membranes with composite layers of nearly zero thickness, ACS Appl. Mater. Interfaces 8 (2016) 21979–21983.

[30] S.Y. Ding, J. Gao, Q. Wang, Y. Zhang, W.G. Song, C.Y. Su, W. Wang, Construction of covalent organic framework for catalysis: Pd/COF-LZU1 in suzuki-miyaura coupling reaction, J. Am. Chem. Soc. 133 (2011) 19816–19822.

[31] X.S. Shi, R. Wang, A.K. Xiao, T.Z. Jia, S.-P. Sun, Y. Wang, Layer-by-layer synthesis of covalent organic frameworks on porous substrates for fast molecular separations, ACS Appl. Nano Mater. 1 (2018) 6320–6326.

[32] R. Wang, X.S. Shi, Z. Zhang, A.K. Xiao, S.-P. Sun, Z.L. Cui, Y. Wang, Unidirectional diffusion synthesis of covalent organic frameworks (COFs) on polymeric substrates for dye separation, J. Membr. Sci. 586 (2019) 274–280.
[33] R. Wang, X.S. Shi, A.K. Xiao, W. Zhou, Y. Wang, Interfacial polymerization of covalent organic frameworks (COFs) on polymeric substrates for molecular separations, J. Membr. Sci. 566 (2018) 197–204.
[34] M.Y. Wu, J.Q. Yuan, H. Wu, Y.L. Su, H. Yang, X.D. You, R.N. Zhang, X.Y. He, N. A. Khan, R. Kasher, Z.Y. Jiang, Ultrathin nanofiltration membrane with polydopamine-covalent organic framework interlayer for enhanced permeability and structural stability, J. Membr. Sci. 576 (2019) 131–141.
[35] H.W. Fan, J.H. Gu, H. Meng, A. Knebel, J. Caro, High-flux membranes based on the covalent organic framework COF-LZU1 for selective dye separation by nanofiltration, Angew. Chem. Int. Ed. 57 (2018) 4083–4087.
[36] H.Y. Li, A.M. Evans, I. Castano, M.J. Strauss, W.R. Dichtel, J.L. Bredas, Nucleation-elongation dynamics of two-dimensional covalent organic frameworks, J. Am. Chem. Soc. 142 (2020) 1367–1374.
[37] S. Karan, Z. Jiang, A. Livingston, Sub-10 nm polyamide nanofilms with ultrafast solvent transport for molecular separation, Science 348 (2015) 1347–1351.
[38] S. Gao, Y. Zhu, Y. Gong, Z. Wang, W. Fang, J. Jin, Ultrathin polyamide nanofiltration membrane fabricated on brush-painted single-walled carbon nanotube network support for ion sieving, ACS Nano 13 (2019) 5278–5290.
[39] Z. Zhang, X.S. Shi, R. Wang, A.K. Xiao, Y. Wang, Ultra-permeable polyamide membranes harvested by covalent organic framework nanofiber scaffolds: a two-in-one strategy, Chem. Sci. 10 (2019) 9077–9083.
[40] Z.Y. Wang, Z.X. Wang, S.H. Lin, H.L. Jin, S.J. Gao, Y.Z. Zhu, J. Jin, Nanoparticle-templated nanofiltration membranes for ultrahigh performance desalination, Nat. Commun. 9 (2018) 2004.